



OPEN

Silver incorporated into $g\text{-C}_3\text{N}_4$ /Alginate as an efficient and heterogeneous catalyst for promoting click and A^3 and KA^2 coupling reaction

Mansoureh Daraie¹, Majid M. Heravi¹✉, Pourya Mohammadi¹ & Ali Daraie²

$\text{Fe}_3\text{O}_4/g\text{-C}_3\text{N}_4$ /Alginate-Ag nanocomposite as a novel and effective nanocatalyst was successfully prepared. This nanocomposite was fully characterized using several techniques such as X-ray diffraction (XRD), field emission scanning electron microscopy with energy dispersive spectroscopy (FESEM-EDS), transmission electron microscopy (TEM), and Fourier transform infrared spectroscopy (FTIR). In addition, the catalytic activity of this novel and characterized nanocatalyst was investigated in the regioselective synthesis of 1,4-disubstituted 1,2,3-triazoles via click reaction and A^3 and KA^2 coupling reaction in aqueous media. The prepared nanocatalyst was simply recovered by using an external magnet and reused for several times with a slight loss of catalytic activity.

Crucial aim of catalytic reactions in organic synthesis is the success in the selective production of target compounds with high efficiency in terms of atom economy and the yield of each reaction step. The ease of separation and recyclability of the catalyst are other noticeable challenges in this field. Hence, researchers try to design new catalysts and examine them in organic reactions to achieve new methodologies¹. They wish to produce the products by these catalyst via green and eco-friendly steps in which minimum amount of toxic reagents or wastes is used or produced, respectively, and the needed energy and the number of reaction steps are reduced. Currently, one-pot reactions and heterogeneous catalysis are the most attractive choices to design new methods for the synthesis of target compounds because this way saves the consuming energy, while separation and purification of the product is simple with no need to isolate the intermediates, and the catalyst is filtered and possibly reused². Besides, the structure of heterogeneous catalysts can be modified with various functions, otherwise diverse functions in a catalyst can work separately or cooperatively in different steps^{3,4}.

Incorporation of metal nanoparticles (NPs) onto a substrate of catalyst has received increased attention in recent years. This is as a result of improvements in catalytic methodologies, particularly by the development of bottom-up approaches. Preparation and stabilization of metal NPs need specific capping organic molecules, including polymers, ligands, and surfactants, to control the NPs size and to prevent agglomeration of particles⁵.

The ways for the preparation of distinct supported metal NPs and innovation of procedures for the isolation and recycling of catalysts are of hot topics in catalytic research. In this regard, researchers have drawn their attention on the design of new supported magnetic NPs based catalysts that can be effortlessly separated from the mixture using magnets⁶.

Lately, magnetic nanoparticles have been applied as excellent supports with a great surface-to-volume ratio led to notable stability, great catalyst loading capability, uniform dispersion, and suitable recycling⁷.

Silver nanoparticles owing to their individual physical and chemical properties are widely used in different fields such as medicine, health, agriculture, animal husbandry, household, electronics, and packaging⁸. One of the principal problems of the usage of the nanoparticles in reactions is related to their aggregation. Stabilization of nanoparticles on proper supports overcomes the problems associated with their stability, separation, and recovery. In this regard, various supports have been utilized for the stabilization of nanoparticles such as zeolite, TiO_2 , graphene oxide, Fe_3O_4 ^{9–12}, and carbon-based supports^{13–17}. Among the different supports, $g\text{-C}_3\text{N}_4$ has shown good chemical resistance^{18–20}.

¹Department of Chemistry, School of Physics and Chemistry, Alzahra University, Tehran, Iran. ²Faculty of Electrical Engineering and Robotic, Shahrood University of Technology, Shahrood, Iran. ✉email: m.heravi@alzahra.ac.ir

1,2,3-Triazole bearing *N*-heterocyclic systems have been used in various fields of chemistry^{21–24}. Even though such structures are not found in natural sources, they are acted as amide-bond surrogates in biologically active compounds owing to their large dipole moment, forming hydrogen bonds, and incredible metabolic stabilities during enzymatic degradation^{25–27}.

The amide-triazole isosteric substitution in 1,2,3-triazole compounds was employed for the synthesis of a wide range of medicinal frameworks having anti-HIV, antibacterial and anticancer activities^{28–32}.

In 2001, Sharpless and Meldal discovered that Copper (I) can regioselectively catalyze alkyne-azide cycloaddition and named briefly it as CuAAC reaction. This reaction was then categorized as the “paradigm” of all “click reactions”^{33–35}.

In order to develop the catalytic synthesis of 1,4-disubstituted 1,2,3-triazoles, some transition metals, including zinc (Zn)^{36,37}, gold (Au)³⁸, and nickel (Ni)³⁹, were also utilized⁴⁰. In 2013, Erick Cuevas demonstrated that AgCl complex catalyzed the formation of 1,2,3-triazoles⁴¹.

One type of the KA² and A³ coupling reactions is the treatment of alkynes with amines and carbonyl compounds. Such coupling reactions are important due to the construction of propargylamines as valuable substrate in the architecture of various organic compounds, including natural products, bioactive nitrogen-rich compounds such as fungicides and herbicides, and heterocyclic structures such as quinolines, pyrroles, and indolizines^{42–46}. Remarkably, KA² and A³ coupling reactions not only are employed in the synthesis of propargylamines, but also are considered as alternatives for the classic synthesis of propargyltriflates and propargylic phosphates. Transition metal based catalysts including Au, Zn, Cu, Ag, and Fe can promote such coupling reactions^{47,48}.

Because of the importance of coupling reactions in art of synthesis, recently researches has been focused on the deletion of their drawbacks, especially by designing nontoxic heterogeneous catalysis^{49–53}.

In attempt to disclose the utility of C₃N₄ as a promising catalyst support for design and synthesis of heterogeneous catalysts^{54–57}, in this work, we claim the preparation and full characterization of Fe₃O₄/g-C₃N₄/Alginate-Ag nanocomposite as an effective and novel nanocatalyst in the regioselective synthesis of 1,4-disubstituted -1,2,3-triazoles via Click^{58–60} and A³ and KA² coupling reactions under mild and environmentally benign conditions.

Experimental

Materials and instruments. The catalyst was synthesized using the following chemical materials: Thiourea, Polyalginate, AgNO₃, NH₃, FeCl₃·6H₂O, FeCl₂·4H₂O and hydrazine hydrate. All purchased from Sigma-Aldrich and used without any purification.

For the synthesis of triazole derivatives and A³ and KA² coupling products, α-haloketones or alkyl halides, terminal alkynes and sodium azide, morpholine or piperidine and different aromatic aldehyde were used. These compounds were obtained from Sigma-Aldrich on analytical grade. The progress of click reaction was monitored by TLC silica gel 60 F254, using ultraviolet light.

To characterize Fe₃O₄-g-C₃N₄-Alginate-Ag, SEM, EDX, XRD, TEM, FTIR, and ICP-AES were employed. FTIR spectra of each hybrid component of catalyst was recorded using KBr disks on FTIR spectrometer Bruker Tensor 27 in the 400–4000 cm⁻¹ region. SEM image of the catalyst was obtained from a FESEM-TESCAN-MIRA3 microscope coupled with EDX (TSCAN). X-ray diffraction (XRD) pattern was achieved by a Co Kα radiation (λ = 1.78897 Å, 40 keV and 40 Ma).

Synthesis of Fe₃O₄-g-C₃N₄-Alginate-Ag magnetic nanocatalyst. *Synthesis of g-S-C₃N₄.* Thiourea (5.0 g) was put into a crucible and then heated at 550 °C and for 3 h. Then, the product (g-C₃N₄) was powdered.

Synthesis of Fe₃O₄-g-C₃N₄. At first, 1.0 g of g-C₃N₄ was added to the 120 mL of H₂O and then was dispersed, after that, Fe³⁺ and Fe²⁺ with molar ratio 2:1 were added to the reaction mixture. Then, it was heated at 55 °C. Next, 10 mL of ammonia solution (28%) was poured to it. This mixture was stirred for 1 h. After the end of reaction, the precipitated was separated by an external magnet, and washed several times with distilled water and ethanol (2:1) and dried at 25 °C for overnight.

Synthesis of Fe₃O₄-g-C₃N₄-Alg-Ag. Typically, 1.0 g of Fe₃O₄-g-C₃N₄ was poured in distilled water (40 mL) and stirred for 30 min. Then 20 mL of the solution of the alginate polymer (1.5%) was added to the above of the reaction mixture. The mixture was stirred at room temperature for 5 h. Then, 30 mL of the AgNO₃ (3 mM) was added. This mixture was stirred for 2 h, after that 0.5 mL diluted hydrazine hydrate was poured and stirred for 24 h. Finally, the magnetic precipitate was collected with an external magnet. The target product washed with distilled water and ethanol (2:1) and dried at 25 °C for overnight. The ICP-AAS analysis was used to the determination of Ag immobilized on the prepared nanocatalyst, that the results showed, 0.9 mmol of Ag loaded in the 1 g of catalyst (Fig. 1).

General procedure for the synthesis of 1,4-disubstituted 1,2,3-triazoles. To a mixture of alkyl halide or α-haloketone (1 mmol), sodium azide (1.2 mmol), and terminal alkyne (1 mmol) in water (5 ml), Fe₃O₄-g-C₃N₄-Alg-Ag (0.02 g) as a catalyst was added and the resulting mixture was magnetically stirred for the appropriate time. At the end of the reaction (monitored by TLC), the solid was filtered off and recrystallized in EtOH (Fig. 2).

Typical procedure of A³ and KA² coupling reaction. 0.02 g of Fe₃O₄-g-C₃N₄-Alg-Ag was poured into a round bottom flask containing an aqueous mixture of alkyne (1.1 mmol), aromatic aldehyde (1 mmol), and

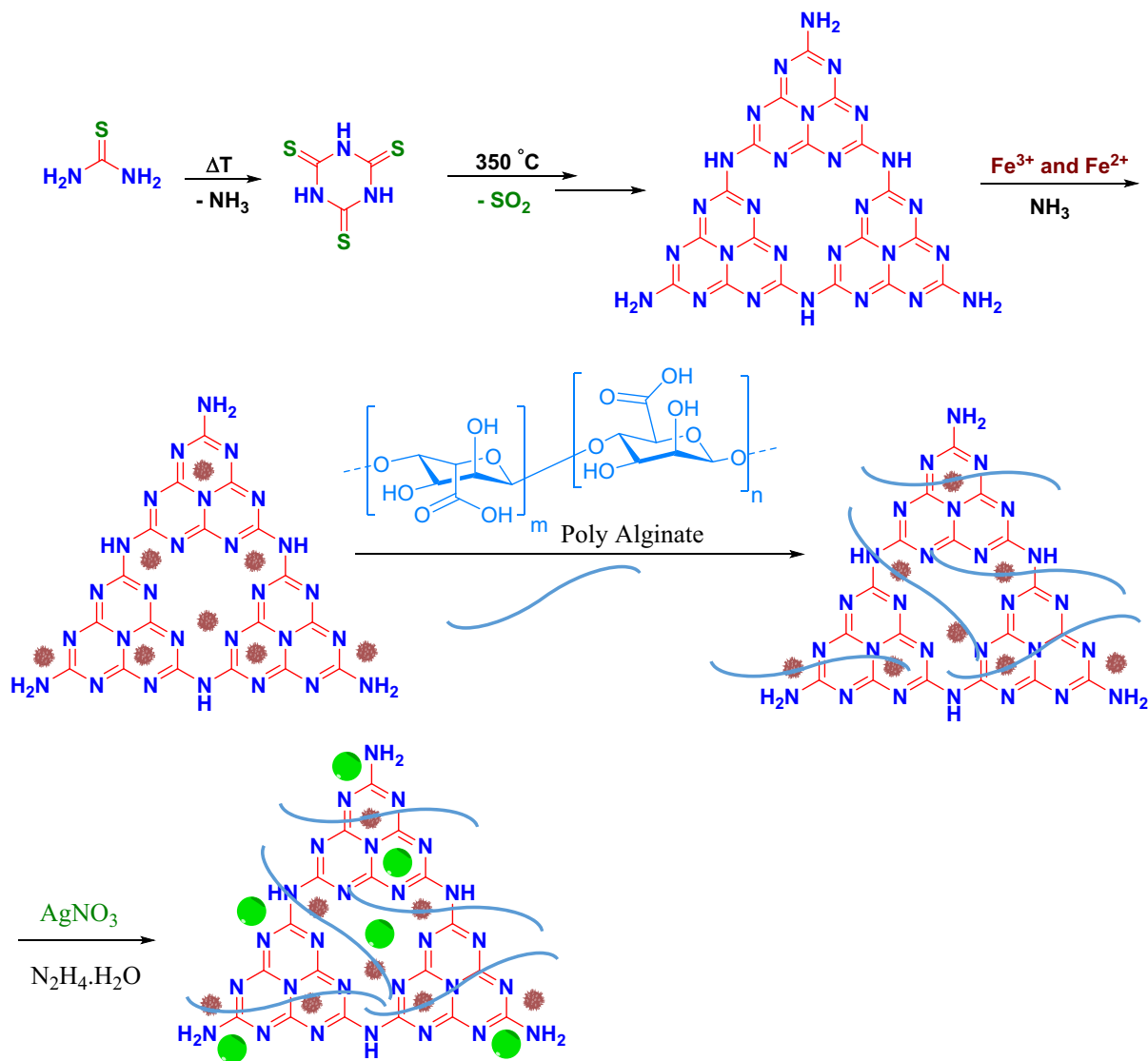


Figure 1. The schematic route for the preparation of $\text{Fe}_3\text{O}_4\text{-g-C}_3\text{N}_4\text{-Alg-Ag}$ catalyst.

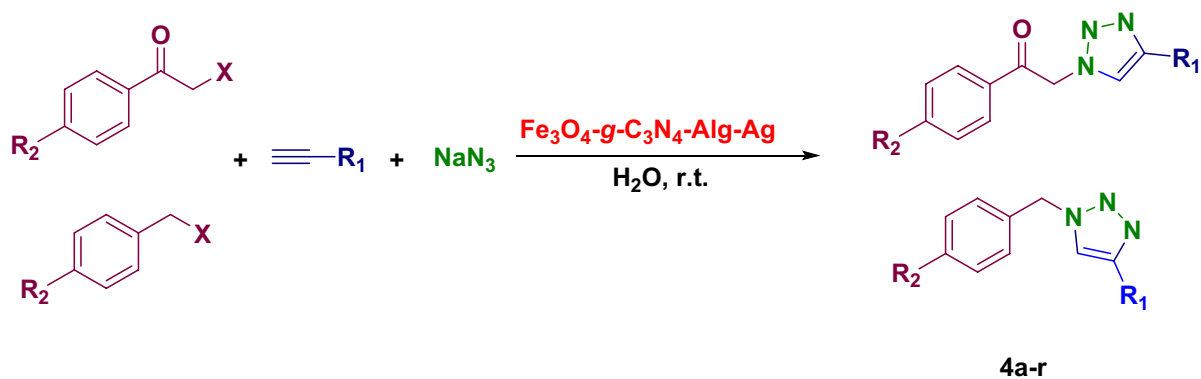


Figure 2. Synthesis of 1,4-disubstituted 1,2,3-triazoles.

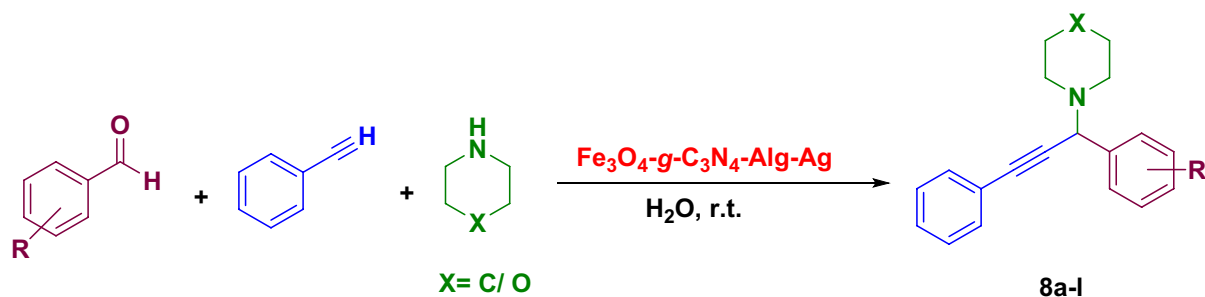


Figure 3. A3 and KA2 coupling reactions.

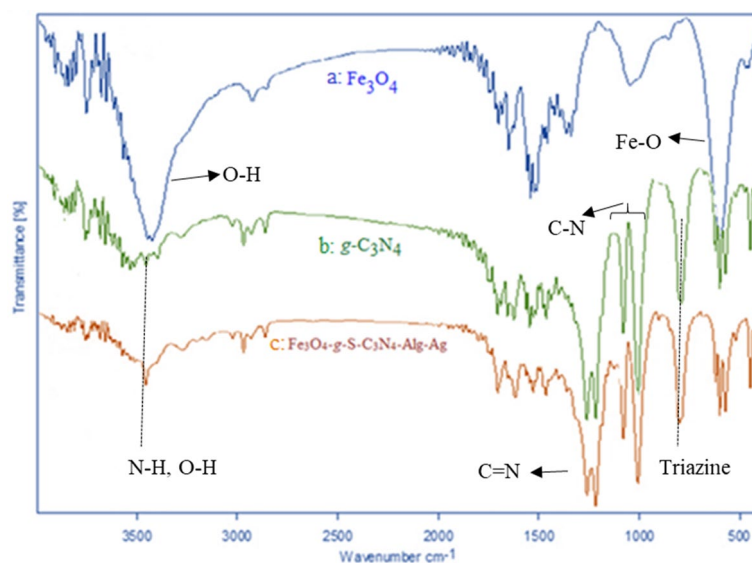


Figure 4. FT-IR spectra of (a) Fe_3O_4 , (b) $\text{g-C}_3\text{N}_4$ and (c) $\text{Fe}_3\text{O}_4\text{-g-C}_3\text{N}_4\text{-Alg-Ag}$ nanomaterials.

piperidine/morpholine (1 mmol). After stirring and heating the reaction mixture for appropriate time, which was monitored by TLC, it was cooled down and filtered (Fig. 3). The crude product comprising catalyst was dissolved in hot EtOH and the residue catalyst was filtered. Then, the filtrate was cooled to give the crystallized pure product.

Result and discussion

Catalyst characterization. FT-IR spectra of $\text{Fe}_3\text{O}_4\text{-g-C}_3\text{N}_4\text{-Alg-Ag}$ nanocatalyst was recorded to detect the functional groups in this catalyst. As shown in Fig. 4a, FT-IR spectrum of Fe_3O_4 displays a strong absorption band at 597 cm^{-1} belonging to the tetrahedral structure of trivalent Fe-O absorption. The hydroxyl groups existing in the Fe_3O_4 surface illustrates a broad band at $3422\text{--}3500\text{ cm}^{-1}$. Figure 4b shows a strong band at 797 cm^{-1} belonging to the special bending vibration of triazine moiety. The bands appeared at the range of 1200 to 1400 cm^{-1} are related to the stretching vibration of C-N group. The peak appeared at 1611 cm^{-1} is due to the stretching vibration of C=N group. In addition, stretching vibration of NH has appeared at 3450 cm^{-1} . FT-IR spectrum of $\text{Fe}_3\text{O}_4\text{-g-C}_3\text{N}_4\text{-Alg-Ag}$ nanostructure is shown in Fig. 4c. As $\text{Fe}_3\text{O}_4\text{-g-C}_3\text{N}_4$ was covered with the polymer, the weak band at 2963 cm^{-1} probably is due to the stretching vibration of aliphatic CH in the polymer structure. Figure 4c shows the FT-IR spectrum of $\text{Fe}_3\text{O}_4\text{-g-C}_3\text{N}_4\text{-Alg-Ag}$ in which there is no change by comparing it with its substrate. $\text{Fe}_3\text{O}_4\text{-g-C}_3\text{N}_4\text{-Alg-Ag}$ is formed after decomposition of Ag NPs on the $\text{Fe}_3\text{O}_4\text{-g-C}_3\text{N}_4\text{-Alg}$, and this spectrum shows the stability of $\text{Fe}_3\text{O}_4\text{-g-C}_3\text{N}_4\text{-Alg}$ during synthesis of Ag NPs.

By using scanning electron microscopy (SEM) the morphology and size of the $\text{Fe}_3\text{O}_4\text{-g-S-C}_3\text{N}_4\text{-Alg-Ag}$ synthesized nanocatalyst were investigated (Fig. 5). The particles almost have a spherical and the average size of them is about 28 nm. Whereas the surface of the $\text{g-C}_3\text{N}_4$ covered with Fe_3O_4 and Ag nanoparticles cannot be observed of theirs.

The EDX analysis as elemental analysis confirmed the presence of Ag, O, Fe, C, S, and N elements which can be confirmed elemental analysis of prepared catalyst (Fig. 6). The EDX-mapping images of synthesized nanocatalyst illustrated in Fig. 7. The elements of Ag, O, Fe, C, S, and N were goodly dispersed into the nanocatalyst.

The XRD technique is as a method for considering crystal structures of the material. The XRD pattern of the $\text{Fe}_3\text{O}_4\text{-g-C}_3\text{N}_4\text{-Alg-Ag}$ nanocatalyst magnetic was illustrated in the Fig. 8.

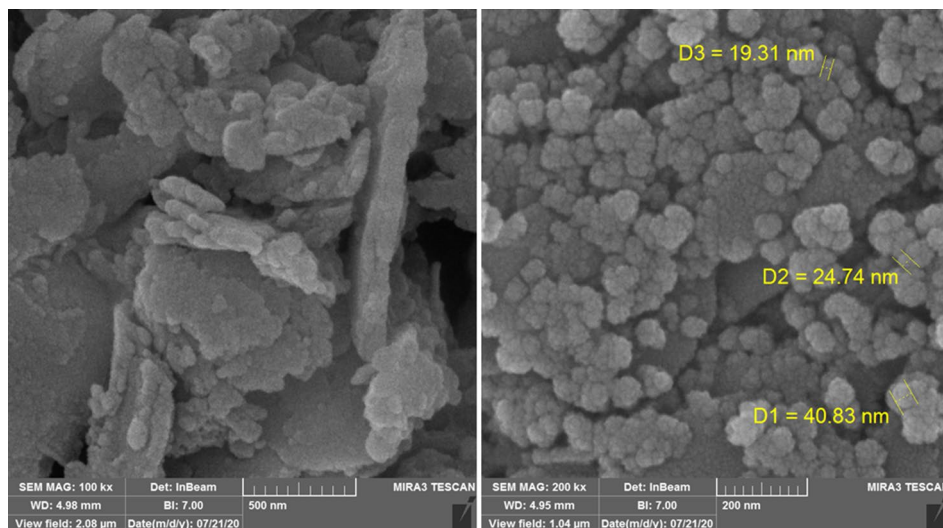


Figure 5. SEM image of Fe_3O_4 -g- C_3N_4 -Alg-Ag nanomaterials.

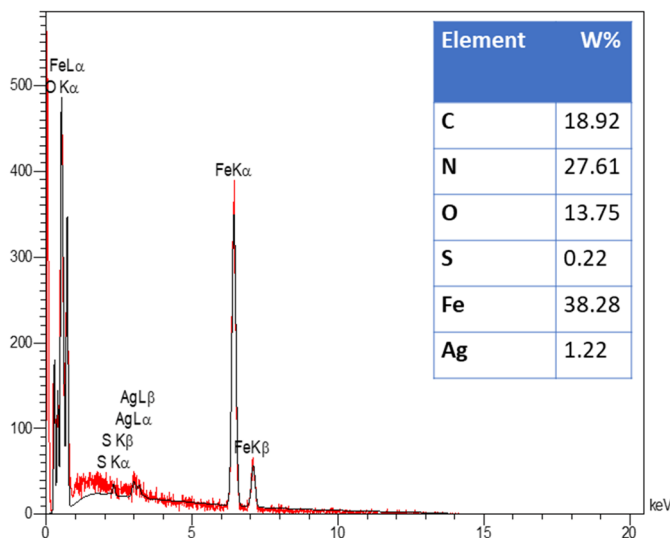


Figure 6. EDX analysis of Fe_3O_4 -g- C_3N_4 -Alg-Ag nanomaterials.

The recorded peaks at $2\theta = 30.1^\circ$, 35.4° , 43.1° , 53.5° , 57.2° , and 62.7° , related to the planes (2 2 0), (3 1 1), (4 0 0), (4 2 2), (5 1 1), and (4 4 0) respectively, that can be confirmed face-centered cubic structure of Fe_3O_4 nanoparticles (JCPDS card no. 19-0629). Also the XRD pattern of Ag nanoparticles shows the peaks at $2\theta = 38.0^\circ$, 44.2° , 64.5° , and 77.5° that can be related to the planes (1 1 1), (2 0 0), (2 2 0) and (3 1 1) respectively, (JCPDS card no. 65-2871), the planes g- C_3N_4 shows a peak at $2\theta = 28^\circ$ (JCPDS card no. 87-1526). This peak confirmed the presence of g- C_3N_4 .

According to the TEM analysis, Fe_3O_4 and Ag nanoparticles were dispersed on the g- C_3N_4 -Alginate. TEM images display the mean size of the particles are about 12 nm. It also shows that g- C_3N_4 sheets are nanoscale (Fig. 9).

Catalytic activity. It was found that this is a potent catalyst in organic transformations. To study this supposition, Fe_3O_4 -g- C_3N_4 -Alginate-Ag was used as catalyst in the Click reaction of sodium azide, α -haloketone or alkyl halide and terminal alkynes for the synthesis of triazoles. Primarily, the reaction of phenylacetylene, benzyl bromide and sodium azide was designated as the model reaction and run in the different solvents and also under solvent-free conditions. Pleasantly, by comparing the yields of the model reactions in different solvents, it was confirmed that water as the best protic solvent gained the highest yield of the desired product. Afterward, to find the optimum reaction temperature and the effective amounts of catalyst, the model reaction was repeated in the presence of various catalyst amounts at different reaction temperatures (Table 1).

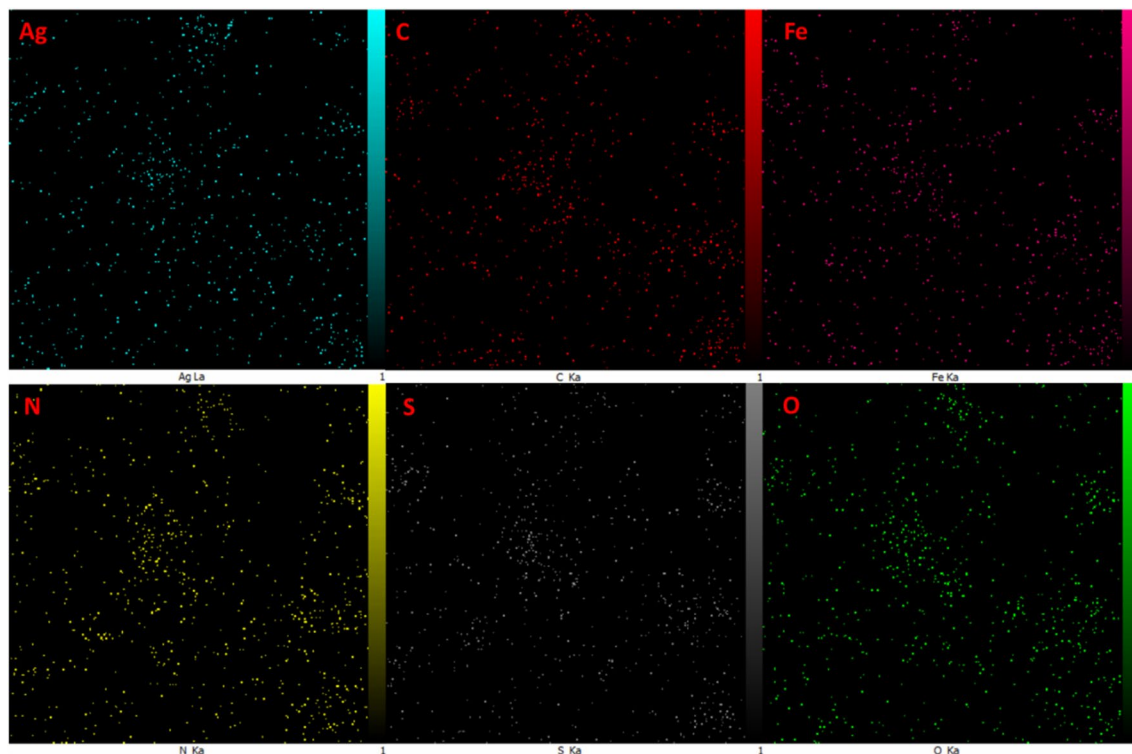


Figure 7. EDX-mapping study of Fe_3O_4 -g- C_3N_4 -Alg-Ag nanomaterials.

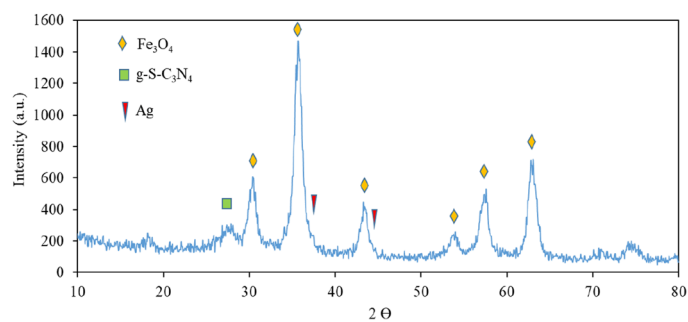


Figure 8. XRD pattern of Fe_3O_4 -g- C_3N_4 -Alg-Ag nanomaterials.

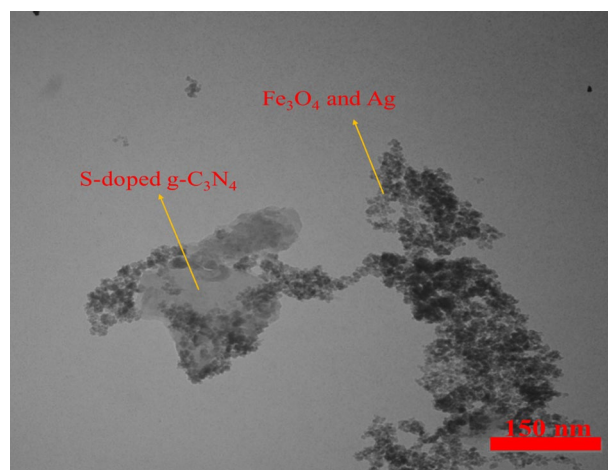


Figure 9. TEM image of the Fe_3O_4 -g- C_3N_4 -Alg-Ag nanomaterials.

Entry	Loading of catalyst (g)	Condition (temp. (°C))	Time (min)	Yield (%)
1	0.02	H ₂ O/r.t.	15	98
2	0.02	H ₂ O/50	12	92
3	0.02	H ₂ O/100	12	94
4	0.02	H ₂ O-EtOH (1:1)/r.t.	20	89
5	0.02	EtOH/r.t.	25	85
6	0.02	CH ₃ CN/r.t.	30	75
7	0.02	CH ₂ Cl ₂ /r.t.	40	70
8	0.02	DMF/r.t.	45	50
9	0.02	Solvent free/r.t.	20	70
10	0.02	Solvent free/80	15	82
11	None	H ₂ O/r.t.	60	30
12	0.01	H ₂ O/r.t.	20	90
13	0.03	H ₂ O/r.t.	15	98
14	0.04	H ₂ O/r.t.	15	97

Table 1. Optimization reaction condition using Fe₃O₄/s-C₃N₄-Starch-Ag As catalyst. Reaction condition: phenylacetylene (1 mmol), benzyl bromide (1 mmol), sodium azide (1.3 mmol), solvent (5 ml).

The results indicated that the highest yield of the model product was achieved at room temperature in the presence of 0.02 g of catalyst. The generality of the protocol was then studied. For this purpose, Various substrates with different electron densities were participated in this reaction under optimum conditions and numerous 1,2,3-triazoles were produced (Table 2). The results proved that Fe₃O₄-g-C₃N₄-Alginate-Ag is a good candidate to catalyze the reactions of different substrates giving the corresponding 1,2,3-triazoles in short reaction times and great yields.

Reaction mechanism. Relied on the preceding reports⁴⁸, a suggested probable mechanistic route for the three-component click reaction in the presence of Fe₃O₄-g-C₃N₄-Alginate-Ag as catalyst is depicted in Fig. 10. Initially, the azide ion is served as a nucleophile group to add to benzyl halide. Instantaneously, the catalyst stimulates the terminal alkyne tolerating homocoupling reaction to attain a diyne. Lastly, the desired product 1,2,3-triazole is provided via CuI-mediated cycloaddition reaction.

Next, we examined the three-component A³ and KA² coupling reactions of aromatic aldehydes, phenyl acetylene and cyclic amine in the presence of Fe₃O₄-g-C₃N₄-Alginate-Ag as a catalyst in H₂O at ambient temperature. The coupling compounds were efficiently obtained in good to excellent yields (Table 3).

Catalyst recyclability. Finally, the recyclability of Fe₃O₄-g-C₃N₄-Alginate-Ag was investigated. In this regard, the product yield in the model product was studied for 6 cycles in the presence of fresh and recycled Fe₃O₄-g-C₃N₄-Alginate-Ag (Fig. 11). The results demonstrated that Fe₃O₄-g-C₃N₄-Alginate-Ag can be recycled for seven reaction runs while its catalytic activity was not reduced.

Conclusion

In this work, Ag nanoparticle immobilized on Fe₃O₄/g-C₃N₄/Alginate was synthesized and applied in Click and A³ and KA² coupling reactions in water as a green solvent. The merits of these reactions are short reaction time, good efficiency and purity. The synthesized nanocatalyst also was readily separated from the reaction mixture

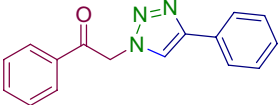
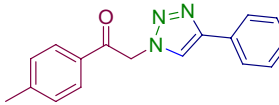
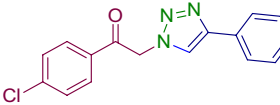
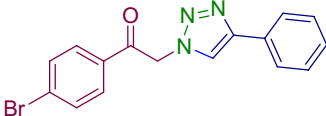
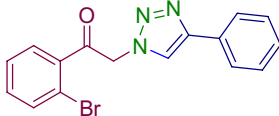
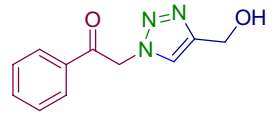
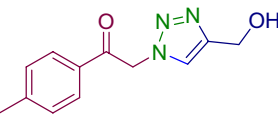
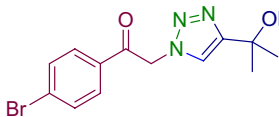
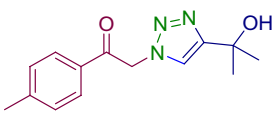
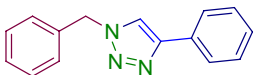
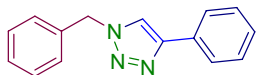
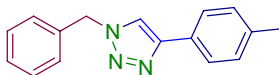
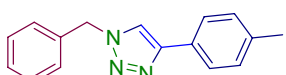
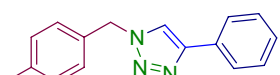
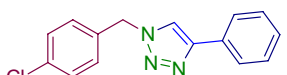
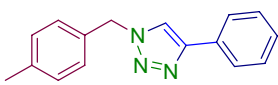
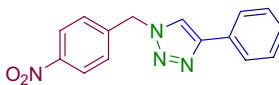
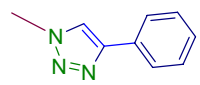
		
4a, X = Br, M. P.= 168-170	4b, X = Br, M. P.= 158-160	4c, X = Br, M. P.= 110-112
		
4d, X = Br, M. P.= 116-118	4e, X = Br, M. P.= 188-190	4f, X = Br, M. P.= 111-114
		
4g, X = Br, M. P.= 182-184	4h, X = Br, M. P.= 154-154	4i, X = Br, M. P.= 166-168
		
4j, X = Cl, M. P.= 126-128	4k, X = Br, M. P.= 127-128	4l, X = Cl, M. P.= 148-150
		
4m, X = Br, M. P.= 147-148	4n, X = Cl, M. P.= 104-106	4o, X = Cl, M. P.= 144-147
		
4p, X = Br, M. P.= 105-107	4q, X = Br, M. P.= 152-155	4r, CH ₃ I, M. P.= 122-125

Table 2. Synthesis of 1,2,3-triazoles in the presence of Fe₃O₄-g-C₃N₄-Alginate-Ag^{52,53}.

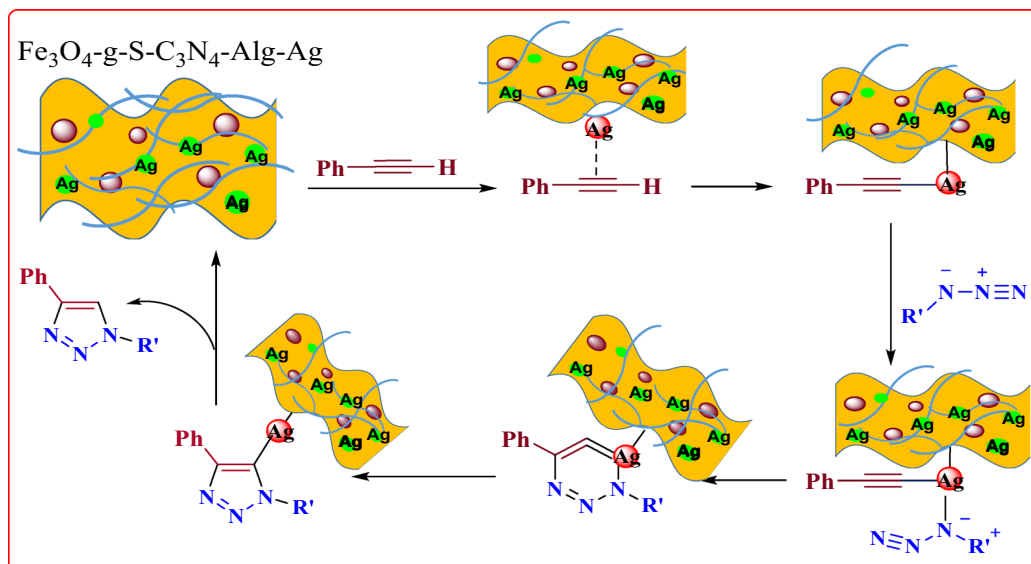


Figure 10. Plausible reaction mechanism.

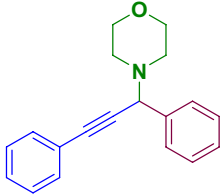
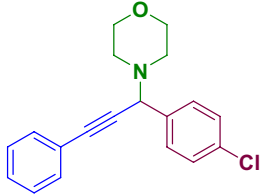
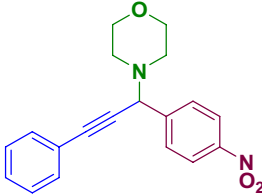
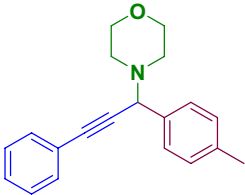
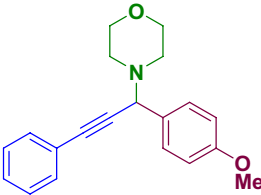
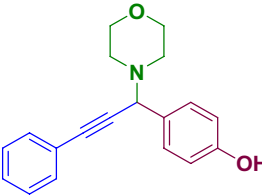
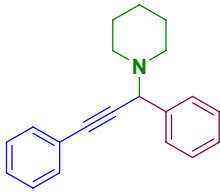
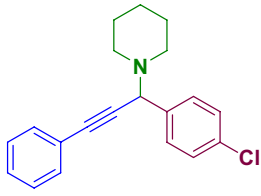
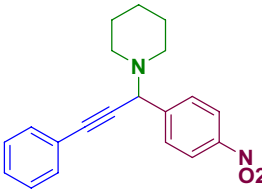
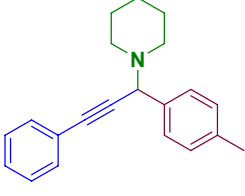
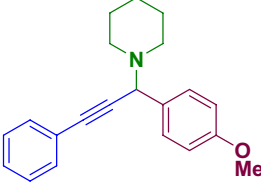
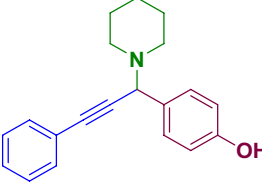
		
8a , M, 15 min, 95%	8b , 20 min, 91%	8c , 22 min, 91%
		
8d , 25 min, 90%	8e , 25 min, 93%	8f , 30 min, 89%
		
8g , 20 min, 91%	8h , 22 min, 94%	8i , 27 min, 93%
		
8j , 30 min, 85%	8k , 30 min, 82%	8l , 35 min, 80%

Table 3. A^3 and KA^2 coupling reactions in the presence of Fe_3O_4 -g- C_3N_4 -Alginate-Ag^{55,56}.

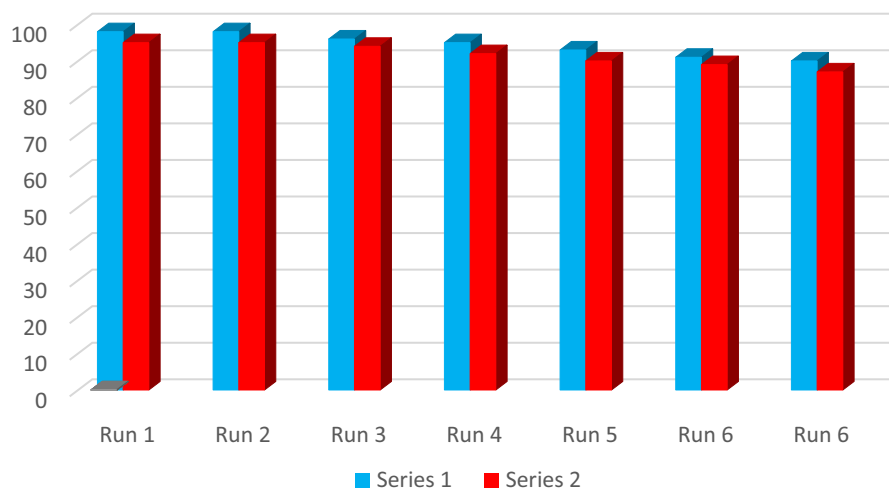


Figure 11. Reusability of $\text{Fe}_3\text{O}_4\text{-g-C}_3\text{N}_4\text{-Alginate-Ag}$.

using an external magnet, washed and reused for several runs without a significant decrease in its activity (Supplementary Information).

Received: 10 April 2021; Accepted: 22 June 2021

Published online: 08 July 2021

References

- Anastas, P. & Eghbali, N. Green chemistry: Principles and practice. *Chem. Soc. Rev.* **39**, 301–312 (2010).
- Nishimura, S., Takagaki, A. & Ebitani, K. Characterization, synthesis and catalysis of hydrotalcite-related materials for highly efficient materials transformations. *Green Chem.* **15**, 2026 (2013).
- Climent, M., Corma, A., Iborra, S. & Sabater, M. Heterogeneous catalysis for tandem reactions. *ACS Catal.* **4**, 870–891 (2014).
- Shimizu, K. Heterogeneous catalysis for the direct synthesis of chemicals by borrowing hydrogen methodology. *Catal. Sci. Technol.* **5**, 1412–1427 (2015).
- Rossi, L., Costa, N., Silva, F. & Gonçalves, R. Magnetic nanocatalysts: Supported metal nanoparticles for catalytic applications. *Nanotechnol. Rev.* **2**, 597–614 (2013).
- Astruc, D., Lu, F. & Aranzaes, J. Nanoparticles as recyclable catalysts: The frontier between homogeneous and heterogeneous catalysis. *Angew. Chem. Int. Ed.* **44**, 7852–7872 (2005).
- Wang, P., Kong, A., Wang, W., Zhu, H. & Shan, Y. Facile preparation of ionic liquid functionalized magnetic nano-solid acid catalysts for acetalization reaction. *Catal. Lett.* **135**, 159–164 (2010).
- Shankar, P. *et al.* A review on the biosynthesis of metallic nanoparticles (gold and silver) using bio-components of microalgae: Formation mechanism and applications. *Enzyme Microb. Technol.* **95**, 28–44 (2016).
- Atarod, M., Nasrollahzadeh, M. & Mohammad Sajadi, S. Euphorbia heterophylla leaf extract mediated green synthesis of Ag/TiO₂ nanocomposite and investigation of its excellent catalytic activity for reduction of variety of dyes in water. *J. Colloid Interface Sci.* **462**, 272–279 (2016).
- Nasrollahzadeh, M., Mohammad Sajadi, S., Rostami-Vartooni, A. & Khalaj, M. Green synthesis of Pd/Fe₃O₄ nanoparticles using Euphorbia condylocarpa M. bieb root extract and their catalytic applications as magnetically recoverable and stable recyclable catalysts for the phosphine-free Sonogashira and Suzuki coupling reactions. *J. Mol. Catal. A Chem.* **396**, 31–39 (2015).
- Wang, L., Xu, S., He, S. & Xiao, F. Rational construction of metal nanoparticles fixed in zeolite crystals as highly efficient heterogeneous catalysts. *Nano Today* **20**, 74–83 (2018).
- Yang, X., Pachfule, P., Chen, Y., Tsumori, N. & Xu, Q. Highly efficient hydrogen generation from formic acid using a reduced graphene oxide-supported AuPd nanoparticle catalyst. *Chem. Commun.* **52**, 4171–4174 (2016).
- Xue, Y. *et al.* Anchoring zero valence single atoms of nickel and iron on graphdiyne for hydrogen evolution. *Nat. Commun.* **9**, 1460 (2018).
- Yu, H. *et al.* Graphdiyne based metal atomic catalysts for synthesizing ammonia.
- Fang, Y., Xue, Y., Hui, L., Yu, H. & Li, Y. Graphdiyne@Janus magnetite for photocatalytic nitrogen fixation. *Angew. Chem.* **60**(6), 3170–3174 (2021).
- Fang, Y. *et al.* Graphdiyne interface engineering: Highly active and selective ammonia synthesis. *Angew. Chem.* **59**(31), 13021–13027 (2020).
- Zhou, W. *et al.* Controllable synthesis of graphdiyne nanoribbons. *Angew. Chem.* **132**(12), 4938–4943 (2020).
- Thomas, A. *et al.* Graphitic carbon nitride materials: Variation of structure and morphology and their use as metal-free catalysts. *J. Mater. Chem.* **18**, 4893 (2008).
- Alduhaish, O. *et al.* Facile synthesis of mesoporous $\alpha\text{-Fe}_2\text{O}_3\text{/g-C}_3\text{N}_4\text{-NCs}$ for efficient bifunctional electro-catalytic activity (OER/ORR). *Sci. Rep.* **9**, 1–10 (2019).
- Xu, Q., Zhu, B., Jiang, C., Cheng, B. & Yu, J. Constructing 2D/2D Fe₂O₃/g-C₃N₄ direct Z-scheme photocatalysts with enhanced H₂ generation performance. *Solar RRL* **2**, 1800006 (2018).
- Chetia, M., Ali, A., Bordoloi, A. & Sarma, D. Facile route for the regioselective synthesis of 1,4-disubstituted 1,2,3-triazole using copper nanoparticles supported on nanocellulose as recyclable heterogeneous catalyst. *J. Chem. Sci.* **129**, 1211–1217 (2017).
- Dehaen, W. *Chemistry of 1,2,3-Triazoles* (Springer International PU, 2016).
- Muller, T. & Bräse, S. Click chemistry finds its way into covalent porous organic materials. *Angew. Chem. Int. Ed.* **50**, 11844–11845 (2011).

24. Chu, C. & Liu, R. Application of click chemistry on preparation of separation materials for liquid chromatography. *Chem. Soc. Rev.* **40**, 2177 (2011).
25. Lau, Y., Rutledge, P., Watkinson, M. & Todd, M. Chemical sensors that incorporate click-derived triazoles. *Chem. Soc. Rev.* **40**, 2848 (2011).
26. Astruc, D., Liang, L., Rapakousiou, A. & Ruiz, J. Click dendrimers and triazole-related aspects: Catalysts, mechanism, synthesis, and functions. A bridge between dendritic architectures and nanomaterials. *Acc. Chem. Res.* **45**, 630–640 (2011).
27. El-Sagheer, A. & Brown, T. Click nucleic acid ligation: Applications in biology and nanotechnology. *Acc. Chem. Res.* **45**, 1258–1267 (2012).
28. Alvarez, R. *et al.* 1,2,3-Triazole-[2,5-bis-O-(tert-butylidimethylsilyl)-.beta.-D-ribofuranosyl]-3'-spiro-5''-(4''-amino-1'',2''-oxathiole 2'',2''-dioxide) (TSAO) analogs: Synthesis and anti-HIV-1 activity. *J. Med. Chem.* **37**, 4185–4194 (1994).
29. Bohacek, R., McMartin, C. & Guida, W. The art and practice of structure-based drug design: A molecular modeling perspective. *Med. Res. Rev.* **16**, 3–50 (1996).
30. Soltis, M. J. *et al.* Identification and characterization of human metabolites of CAI [5-amino-1-1 (4'-chlorobenzoyl-3,5-dichlorobenzyl)-1,2,3-triazole-4-carboxamide. *Drug Metab. Dispos.* **24**(7), 799–806 (1996).
31. Huisgen, R., Szeimies, G. & Möbius, L. 1.3-Dipolare Cycloadditionen, XXXII. Kinetik der Additionen organischer Azide an CC-Mehrfachbindungen. *Chem. Ber.* **100**, 2494–2507 (1967).
32. Bastide, J., Bonnetot, B., Létouffé, J. & Claudy, P. Polymorphisme de l'hydrure de magnésium sous haute pression. *Mater. Res. Bull.* **15**, 1779–1787 (1980).
33. Meldal, M. & Tornøe, C. Cu-catalyzed azide-alkyne cycloaddition. *Chem. Rev.* **108**, 2952–3015 (2008).
34. Spiteri, C. & Moses, J. Copper-catalyzed azide-alkyne cycloaddition: Regioselective synthesis of 1,4,5-trisubstituted 1,2,3-triazoles. *Angew. Chem. Int. Ed.* **49**, 31–33 (2009).
35. John, J., Thomas, J. & Dehaen, W. Organocatalytic routes toward substituted 1,2,3-triazoles. *Chem. Commun.* **51**, 10797–10806 (2015).
36. Sultana, J. & Sarma, D. Ag-catalyzed azide-alkyne cycloaddition: Copper free approaches for synthesis of 1,4-disubstituted 1,2,3-triazoles. *Catal. Rev.* **62**, 96–117 (2019).
37. Meng, X., Xu, X., Gao, T. & Chen, B. Zn/C-catalyzed cycloaddition of azides and aryl alkynes. *Eur. J. Org. Chem.* **2010**, 5409–5414 (2010).
38. Paplal, B., Nagaraju, S., Sridhar, B. & Kashinath, D. Regioselective synthesis of functionalized 1,2,3-triazoles via oxidative [3+2]-cycloaddition using Zn(OAc)₂-tBuOOH or ZnO nanoparticle as catalyst system in aqueous medium. *Catal. Commun.* **99**, 115–120 (2017).
39. Morozova, M. *et al.* Regioselective Zn(OAc)₂-catalyzed azide-alkyne cycloaddition in water: The green click-chemistry. *Org. Chem. Front.* **4**, 978–985 (2017).
40. Surya Prakash Rao, H. & Chakibanda, G. Raney Ni catalyzed azide-alkyne cycloaddition reaction. *RSC Adv.* **4**, 46040–46048 (2014).
41. Díaz Arado, O. *et al.* On-surface azide-alkyne cycloaddition on Au(111). *ACS Nano* **7**, 8509–8515 (2013).
42. Boominathan, M. *et al.* Nanoporous titania-supported gold nanoparticle-catalyzed green synthesis of 1,2,3-triazoles in aqueous medium. *ACS Sustain. Chem. Eng.* **1**, 1405–1411 (2013).
43. Ortega-Arizmendi, A., Aldeco-Pérez, E. & Cuevas-Yañez, E. Alkyne-azide cycloaddition catalyzed by silver chloride and “abnormal” silverN-heterocyclic carbene complex. *Sci. World J.* **2013**, 1–8 (2013).
44. Albaladejo, M., Alonso, F., Moglie, Y. & Yus, M. Three-component coupling of aldehydes, amines, and alkynes catalyzed by oxidized copper nanoparticles on titania. *Eur. J. Org. Chem.* **2012**, 3093–3104 (2012).
45. Villaverde, G., Corma, A., Iglesias, M. & Sánchez, F. Heterogenized gold complexes: Recoverable catalysts for multicomponent reactions of aldehydes, terminal alkynes, and amines. *ACS Catal.* **2**, 399–406 (2012).
46. Katkar, S. & Jayaram, R. Cu–Ni bimetallic reusable catalyst for synthesis of propargylamines via multicomponent coupling reaction under solvent-free conditions. *RSC Adv.* **4**, 47958–47964 (2014).
47. Salam, N. *et al.* Cu-grafted mesoporous organic polymer: A new recyclable nanocatalyst for multi-component, N-arylation and S-arylation reactions. *Catal. Sci. Technol.* **3**, 3303 (2013).
48. Satyanarayana, K., Ramaiah, P., Murty, Y., Chandra, M. & Pammi, S. Recyclable ZnO nano particles: Economical and green catalyst for the synthesis of A3 coupling of propargylamines under solvent free conditions. *Catal. Commun.* **25**, 50–53 (2012).
49. Bobadilla, L., Blasco, T. & Odriozola, J. Gold(iii) stabilized over ionic liquids grafted on MCM-41 for highly efficient three-component coupling reactions. *Phys. Chem. Chem. Phys.* **15**, 16927 (2013).
50. Hosseini-Sarvari, M. & Moeini, F. Nano copper(i) oxide-zinc oxide catalyzed coupling of aldehydes or ketones, secondary amines, and terminal alkynes in solvent-free conditions. *New J. Chem.* **38**, 624–635 (2014).
51. Borah, B., Borah, S., Saikia, K. & Dutta, D. Efficient one-pot synthesis of propargylamines catalysed by gold nanocrystals stabilized on montmorillonite. *Catal. Sci. Technol.* **4**, 4001–4009 (2014).
52. Zeng, T. *et al.* Fe₃O₄ nanoparticles: A robust and magnetically recoverable catalyst for three-component coupling of aldehyde, alkyne and amine. *Green Chem.* **12**, 570 (2010).
53. Hui, T., Cui, J. & Wong, M. Modular synthesis of propargylamine modified cyclodextrins by a gold(iii)-catalyzed three-component coupling reaction. *RSC Adv.* **7**, 14477–14480 (2017).
54. Sadjadi, S., Heravi, M. & Daraie, M. A novel hybrid catalytic system based on immobilization of phosphomolybdic acid on ionic liquid decorated cyclodextrin-nanosponges: Efficient catalyst for the green synthesis of benzochromeno-pyrazole through cascade reaction: Triply green. *J. Mol. Liq.* **231**, 98–105 (2017).
55. Sadjadi, S., Heravi, M. & Daraie, M. Cyclodextrin nanosponges: A potential catalyst and catalyst support for synthesis of xanthenes. *Res. Chem. Intermed.* **43**, 843–857 (2016).
56. Sadjadi, S., Heravi, M. & Malmir, M. Pd@HNTs-CDNS-g-C₃N₄: A novel heterogeneous catalyst for promoting ligand and copper-free Sonogashira and Heck coupling reactions, benefits from halloysite and cyclodextrin chemistry and g-C₃N₄ contribution to suppress Pd leaching. *Carbohydr. Polym.* **186**, 25–34 (2018).
57. Mohammadi, P., Heravi, M. & Sadjadi, S. Green synthesis of Ag NPs on magnetic polyallylamine decorated g-C₃N₄ by Heracleum persicum extract: Efficient catalyst for reduction of dyes. *Sci. Rep.* **10**, 1–10 (2020).
58. Daraie, M. & Heravi, M. A biocompatible chitosan-ionic liquid hybrid catalyst for regioselective synthesis of 1,2,3-triazols. *Int. J. Biol. Macromol.* **140**, 939–948 (2019).
59. Hashemi, E., Beheshtiha, Y., Ahmadi, S. & Heravi, M. In situ prepared CuI nanoparticles on modified poly(styrene-co-maleic anhydride): An efficient and recyclable catalyst for the azide-alkyne click reaction in water. *Transition Met. Chem.* **39**, 593–601 (2014).
60. Nemati, F., Heravi, M. & Elhampour, A. Magnetic nano-Fe₃O₄@TiO₂/Cu₂O core-shell composite: An efficient novel catalyst for the regioselective synthesis of 1,2,3-triazoles using a click reaction. *RSC Adv.* **5**, 45775–45784 (2015).
61. Sadjadi, S., Hosseinejad, T., Malmir, M. & Heravi, M. Cu@furfural imine-decorated halloysite as an efficient heterogeneous catalyst for promoting ultrasonic-assisted A3 and KA2 coupling reactions: A combination of experimental and computational study. *New J. Chem.* **41**, 13935–13951 (2017).

Acknowledgements

M. Daraie and M. M. Heravi are grateful to Iran National Science Foundation (INSF) for financial support provided by the post-doctoral project (98010184). We also appreciate Alzahra University University Research Council for their help and supports.

Author contributions

M.D. and P.M. designed the experiments, and P.M. performed the experiments, M.M.H contributed materials/analysis tools, M.D. and P.M. wrote the paper and A.D prepared figures and tables. All authors reviewed the manuscript.

Competing interests

The authors declare no competing interests.

Additional information

Supplementary Information The online version contains supplementary material available at <https://doi.org/10.1038/s41598-021-93239-z>.

Correspondence and requests for materials should be addressed to M.M.H.

Reprints and permissions information is available at www.nature.com/reprints.

Publisher's note Springer Nature remains neutral with regard to jurisdictional claims in published maps and institutional affiliations.



Open Access This article is licensed under a Creative Commons Attribution 4.0 International License, which permits use, sharing, adaptation, distribution and reproduction in any medium or format, as long as you give appropriate credit to the original author(s) and the source, provide a link to the Creative Commons licence, and indicate if changes were made. The images or other third party material in this article are included in the article's Creative Commons licence, unless indicated otherwise in a credit line to the material. If material is not included in the article's Creative Commons licence and your intended use is not permitted by statutory regulation or exceeds the permitted use, you will need to obtain permission directly from the copyright holder. To view a copy of this licence, visit <http://creativecommons.org/licenses/by/4.0/>.

© The Author(s) 2021